A&A 609, A48 (2018)
DOI: 10.1051/0004-6361/201731711

Astronomy & Astrophysics

Fossil group origins

VIII. RX J075243.6+455653 a transitionary fossil group

J. A. L. Aguerri[1,2], A. Longobardi[3,4], S. Zarattini[5,6], A. Kundert[7], E. D'Onghia[7], and L. Domínguez-Palmero[1,8]

[1] Instituto de Astrofísica de Canarias, C/vía Láctea s/n, 38200 La Laguna, Spain
e-mail: jalfonso@iac.es
[2] Departamento de Astrofísica, Universidad de La Laguna, 38206 La Laguna, Spain
[3] Kavli Institute for Astronomy and Astrophysics, Peking University, 5 Yiheyuan Road, Haidian District, Beijing 100871, PR China
[4] Max-Planck-Institut für Extraterrestrische Physik, Giessenbachstrasse, 85741 Garching, Germany
[5] Dipartimento di Fisica, Università degli Studi di Trieste, via Tiepolo 11, 34143 Trieste, Italy
[6] INAF–Osservatorio Astronomico di Trieste, via Tiepolo 11, 34143 Trieste, Italy
[7] Department of Astronomy, University of Wisconsin-Madison, 475 N. Charter St., Madison, WI 53706, USA
[8] Isaac Newton Group of Telescopes, Apartado 321, 38700 Santa Cruz de La Palma, Canary Islands, Spain

Received 4 August 2017 / Accepted 7 October 2017

ABSTRACT

Context. It is thought that fossil systems are relics of structure formation in the primitive Universe. They are galaxy aggregations that have assembled their mass at high redshift with few or no subsequent accretion. Observationally these systems are selected by large magnitude gaps between their 1st and 2nd ranked galaxies (Δm_{12}). Nevertheless, there is still debate over whether or not this observational criterium selects dynamically evolved ancient systems.
Aims. We have studied the properties of the nearby fossil group RX J075243.6+455653 in order to understand the mass assembly of this system.
Methods. Deep spectroscopic observations allow us to construct the galaxy luminosity function (LF) of RX J075243.6+455653 down to $M_r^* + 6$. The analysis of the faint-end of the LF in groups and clusters provides valuable information about the mass assembly of the system. In addition, we have analyzed the nearby large-scale structure around this group.
Results. We identified 26 group members within $r_{200} \sim 0.96$ Mpc. These galaxies are located at $V_c = 15551 \pm 65$ km s^{-1} and have a velocity dispersion of $\sigma_c = 333 \pm 46$ km s^{-1}. The X-ray luminosity of the group is $L_X = 2.2 \times 10^{43}\ h_{70}^{-2}$ erg s^{-1}, resulting in a mass of $M = 4.2 \times 10^{13}\ h_{70}^{-1}\ M_\odot$ within $0.5r_{200}$. The group has $\Delta m_{12} = 2.1$ within $0.5r_{200}$, confirming the fossil nature of this system. RX J075243.6+455653 has a central brightest group galaxy (BGG) with $M_r = -22.67$, one of the faintest BGGs observed in fossil systems. The LF of the group shows a flat faint-end slope ($\alpha = -1.08 \pm 0.33$). This low density of dwarf galaxies is confirmed by the low value of the dwarf-to-giant ratio ($DGR = 0.99 \pm 0.49$) for this system. Both the lack of dwarf galaxies and the low luminosity of the BGG suggests that RX J075243.6+455653 still has to accrete mass from its nearby environment. This mass accretion will be achieved because it is the dominant structure of a rich environment formed by several groups of galaxies (15) within ~7 Mpc from the group center and with ±1000 km s^{-1}.
Conclusions. RX J075243.6+455653 is a group of galaxies that has not yet completed the process of its mass assembly. This new mass accretion will change the fossil state of the group. This group is an example of a galaxy aggregation selected by a large magnitude gap but still in the process of the accretion of its mass.

Key words. galaxies: clusters: general

1. Introduction

The structure formation in the Universe is driven by mergers and accretion of small substructures into larger ones (White & Rees 1978), and these processes are still active at present. Nevertheless, a fraction of the structures present today could be relics of the primitive Universe. These systems are called fossil groups (FG) or, more generically, fossil systems (FS). These ancient galaxy aggregations were formed at high redshift ($z > 1$) with few or no subsequent accretion (D'Onghia et al. 2005). But, do these objects really exist today? Are there systems in the Universe for which the hierarchical formation is frozen since several Gyr ago? If this kind of system exists, they are important because they contain valuable information about the assembly of massive halos in the primitive Universe. We can therefore understand the formation processes that occurred several Gyr ago by analyzing the properties of nearby FSs.

Ponman et al. (1994) established that the group RX J1340.6+4018 was the remnant of an ancient system of galaxies. This system shows extended X-ray emission, indicating that the group is embedded in a massive dark matter halo. In addition, its light is dominated by a central early-type galaxy. The 2nd ranked luminous galaxy belonging to the group is more than 2 mag fainter than the brightest one. The lack of L^* galaxies in the system was interpreted as the result of the central galaxy cannibalizing the surrounding luminous objects over time. These characteristics made this system a candidate for an early-formed and relaxed structure, and it was classified as a fossil relic.

After the discovery of RX J1340.6+4018, other systems were observed with large magnitude gaps between their 1st and 2nd ranked galaxies (Δm_{12}). The presence of a large Δm_{12} in those systems was interpreted as indication of fossilness. Jones et al. (2003) gave the first observational definition of FSs as those galaxy aggregations with $\Delta m_{12} > 2.0$ mag in the r-band

for the galaxies of the systems within half its virial radius. In addition, the central galaxy should be surrounded by an extended diffuse X-ray halo with $L_X > 10^{42}\ h_{50}^{-2}$ erg s^{-1}. This definition was slightly modified by Dariush et al. (2010) according to the analysis of cosmological simulations. They claim that the magnitude gap between the 1st and 4th ranked galaxies of the system ($\Delta m_{1,4}$) was a better quantity to select old and dynamically relaxed galaxy aggregations. In particular, they proposed that fossil systems are those with $\Delta m_{1,4} > 2.5$ for galaxies within half of their virial radius.

Several samples containing fossil candidates have been selected during the last decade in different galaxy surveys based on large values of their Δm_{12} (e.g., Khosroshahi et al. 2007; Santos et al. 2007; Voevodkin et al. 2010; Proctor et al. 2011; Harrison et al. 2012). Many works have obtained the observational properties of these systems. These properties can be grouped in (i) properties of the hot intracluster component; (ii) properties of the central dominant galaxy or the brightest group galaxy (hereafter BGG); and (iii) properties of the galaxy satellite population.

The global X-ray scaling relations of dark matter halos are related to their formation. Halos formed early should have some imprints in their X-ray properties. In particular, more concentrated dark matter halos collapse first in the hierarchical scenario, which can produce a greater compression of the gas in the central regions of the halo and enhance the X-ray temperature (T_X) and luminosity (L_X). Some works suggest that X-ray global scaling relations in FS and non-FS are different. In particular, FSs were found to have larger T_X than non-fossil ones (e.g., Khosroshahi et al. 2007). These differences between FS and non-FS were also reported in scaling relations combining optical and X-ray quantities, such as the $L_X - L_{opt}$ or $L_X - \sigma$ relations (e.g., Proctor et al. 2011; Khosroshahi et al. 2014); they were interpreted as an indication that the halos of FSs formed early in the high redshift Universe. Nevertheless, larger samples of FSs and non-FSs have obtained that those differences do not exist, indicating that according to the global scaling relations, fossil and non-fossil halos are similar (e.g., Harrison et al. 2012; Girardi et al. 2014; Kundert et al. 2015).

The expected early formation in FSs, with no later accretion, should also produce some peculiarities in the observational properties of their BGGs. In particular, their formation at high redshift could be driven by mergers with large amounts of gas (wet mergers). Khosroshahi et al. (2006) reported differences in the isophotes shape between the BGGs in FS and non-FS pointing towards a formation via wet mergers. They obtained that BGGs of FSs have more disky isophotes than those in non-FSs. Nevertheless, these differences in the isophotal shape were not confirmed by other samples of galaxies (Méndez-Abreu et al. 2012). Indeed, the scaling relations of BGGs in FSs show that they assembled a fraction of their mass by wet mergers probably at high redshift. However, a significant fraction of their mass was accreted via later dry mergers (Méndez-Abreu et al. 2012). The similar properties of the stellar populations of BGGs in FSs and non-FSs also point toward a similar formation (La Barbera et al. 2009; Eigenthaler & Zeilinger 2013; Trevisan et al. 2017). Nevertheless, the merging process in the BGGs of FSs has been especially effective because these galaxies are among the brightest galaxies observed in the Universe (Aguerri et al. 2011; Méndez-Abreu et al. 2012; Zarattini et al. 2014).

The galaxy population of FSs and non-FSs are clearly different in the bright-end of the galaxy luminosity function (LF). In particular, FSs show a lack of L^* galaxies (e.g., Khosroshahi et al. 2006; Mendes de Oliveira et al. 2006; Aguerri et al. 2011; Adami et al. 2012; Lieder et al. 2013; Khosroshahi et al. 2014; Zarattini et al. 2014). Additionally, there is also evidence for differences in the number of low-mass galaxies – FSs show LFs with shallower faint-end than non-FSs (Zarattini et al. 2015). This lack of substructure in fossil halos has been interpreted as a challenge for the hierarchical formation (D'Onghia & Lake 2004); nevertheless, this is still a puzzle and a matter of debate (Zibetti et al. 2009). The galaxy population in FSs also shows evidence of substructure similar to non-FSs, arguing against the relaxed and old dynamical age of FSs (Zarattini et al. 2016).

The previously reported properties indicate that selection of systems by only a large magnitude gap does not guarantee the selection of galaxy aggregations that are dynamically old, early forming, and with few subsequent accretions. This has also been pointed out by some numerical cosmological simulations that analyzed the properties of systems with large magnitude gaps. von Benda-Beckmann et al. (2008) showed that the fossilness of a system is a transition phase, whereby galaxy groups and clusters could pass several times through a fossil phase along their evolution. Recently, Kundert et al. (2017) found that, on average, the fossilness of a system changes over 2−3 Gyr. Some simulations also show that the last major merger in BGGs in FSs has occurred more recently than in similar galaxies in non-FSs (Díaz-Giménez et al. 2008; Kundert et al. 2017). The orbital structure of the galaxies in FSs increases the efficiency of mergers into the BGGs in FSs more than in non-FSs (Sommer-Larsen 2006). This produces FSs BGGs that are more massive on average than those in non-FSs (Kundert et al. 2017). Simulations also show that there are differences at the faint-end of the LF between FSs and non-FSs. Thus, Gozaliasl et al. (2014) obtained that there was almost no evolution in the faint-end LF in FSs since $z \sim 1$. In contrast, non-FSs show a strong evolution of the faint-end. Kundert et al. (2017) demonstrated that the most important difference between FSs and non-FSs is related with the halo mass accretion history over the past few Gyr. This difference in the last fraction of the accretion of the mass could be related with the surrounding large-scale environment (Díaz-Giménez et al. 2011). It is likely that a combination of the magnitude gap with other parameters provides a better selection of dynamically old systems. According to Raouf et al. (2014) the combination of the magnitude gap and the luminosity of the central BGG is one of the solutions to obtain dynamically old structures.

The present paper is part of the Fossil Group Origins (FOGO) project. This project aims at a multiwavelength characterization of a large sample of FSs (see Aguerri et al. 2011). We have analyzed so far the properties of their (i) dark matter halos (Girardi et al. 2014; Kundert et al. 2015), (ii) the central BGGs (Méndez-Abreu et al. 2012; Zarattini et al. 2014), and (iii) the galaxy populations (Zarattini et al. 2015, 2016). These observational properties have been compared with state-of-the-art cosmological simulations (Kundert et al. 2017). In the present work we have obtained deep spectroscopic data of the fossil group RX J075243.6+455653 down to $\sim M_r^* + 6$. We have analyzed the properties of this group focusing on the faint-end of its galaxy LF and its large-scale nearby structure. As reported by Raouf et al. (2014), this group has the properties to be an old and evolved galaxy aggregation. In particular, it shows $\Delta m_{12} > 2.0$ and one of the faintest BGGs ($M_r = -22.67$) observed in FSs (Zarattini et al. 2014).

The paper is organized as follows. Section 2 shows the data used. The results are presented in Sect. 3. The discussion

and conclusions are given in Sects. 4 and 5, respectively. Through this paper we have used the cosmology given by H_0 = 70 km s^{-1} Mpc^{-1}, Ω_Λ = 0.7, and Ω_m = 0.3. Using this cosmology, RX J075243.6+455653 is located at a distance of 230.6 Mpc, resulting in a scale of 1.01 kpc arcsec^{-1}.

2. The data for RX J075243.6+455653

We downloaded the photometric and velocity information for galaxy selected objects from Sloan Digital Sky Survey data release 6 (SDSS-DR6; Adelman-McCarthy et al. 2008) within a radius of 4 Mpc around the coordinates α(J2000) = $07^h52^m44.2^s$ and δ(J2000) = +45°56′57.4″. These central coordinates correspond to the peak of X-ray emission detected from the ROSAT satellite and are associated with the group RX J075243.6+455653. This central X-ray peak has a luminosity of $L_X = 2.20 \times 10^{43}$ erg s^{-1} (Zarattini et al. 2014).

The catalog turned out to have 89 galaxies brighter than $m_r \sim 18.0$ with measured radial velocities. Using this data-set from SDSS-DR6, Zarattini et al. (2016) reported that the mean velocity of group (V_c) was 15498 km s^{-1}, and the velocity dispersion σ_c = 259 km s^{-1}. The estimate of L_X allowed us to calculate r_{200} = 0.96 Mpc (Zarattini et al. 2014) using the relations from Böhringer et al. (2007) and Arnaud et al. (2005). The mass of the system was obtained following Girardi et al. (1998) and Girardi & Mezzetti (2001) resulting in $M = 4.2 \times 10^{13}\ M_\odot$ (Zarattini et al. 2014).

The photometric catalog acquired from SDSS-DR6 was used to select targets for additional multi-object spectroscopy with different instruments. In particular, we selected those galaxies with $g - r < 1.1$, $m_r < 19.5$ and within 0.5° (~1.8 Mpc radius at the distance of the group) from the group center to be observed with the AF2 at WHT instrument. These objects will be referred to as spectroscopic targets. A total of 129 spectroscopic targets were selected and located in two AF2 fiber configurations. We obtained low-resolution spectra (R = 280 and grism R158B) in three exposures of 1800 s per pointing, with the spectra reaching $S/N > 5$ for a secure redshift determination (see e.g., Agulli et al. 2016). We also selected targets with $g-r < 1.1$ and $19.5 < m_r < 21.0$ to be observed with the OSIRIS at GTC instrument. A total of 121 spectroscopic targets were located in nine different OSIRIS pointings within r_{200}. In this case the low-resolution spectra (R = 360) of these objects were obtained using the grism R300B in three exposures of 1200 s for each pointing. These new observations consisted of a total of 250 new spectra.

The new spectroscopic data was reduced using different pipelines. The reduction of the data from AF2 at WHT was achieved with the instrument pipeline, version 3.0 (see Domínquez Palmero et al. 2014). In contrast, the data from OSIRIS at GTC was reduced by using the GTCMOS pipeline[1].

2.1. Velocity determination and spectroscopic completeness

The recessional velocities of the new spectra were obtained using rvsao.xcsao IRAF task (see Kurtz et al. 1992). This task cross-correlates a template spectrum library with the observed galaxy spectrum. In this case we have used as template library the one given by Kennicutt (1992). A total of 191 new velocities were determined by this technique. This makes a total of 280 galaxies with measured radial velocities within 4 Mpc from the group center.

[1] http://www.inaoep.mx/~ydm/gtcmos/mos_reduction.html

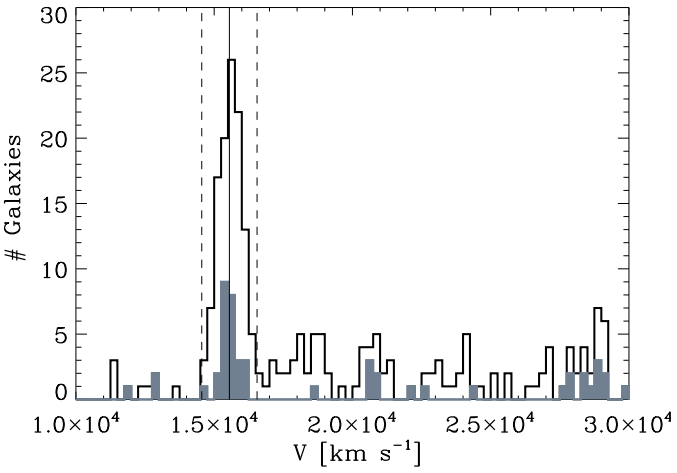

Fig. 1. Velocity histogram of the galaxies in the direction of RX J075243.6+455653. The black histogram shows the radial velocities of the galaxies within 4 Mpc from the cluster center. The gray filled histogram corresponds to galaxies within r_{200}. The vertical line shows the mean velocity of the group. The dashed vertical lines are located at $\pm 3\sigma_c$ from V_c.

Figure 1 shows the velocity histogram of the galaxies in the direction of RX J075243.6+455653 and within an aperture of 4 Mpc. A prominent peak can be observed at $V_c \sim$ 15 550 km s^{-1} which corresponds to the mean velocity of the group (see Zarattini et al. 2014). The velocity histogram also shows that the peak in velocity corresponding to the group is not isolated. In contrast, there is a continuum of background galaxies at larger velocities. The lack of isolation of this group can also be seen by the large number of galaxies with velocities $V_c \pm 3\sigma_c$ out from r_{200} (see Fig. 1). This suggest that the group is surrounded by other galaxies or groups.

The group members were determined by using a simple σ-clipping algorithm. Thus, we computed several times the mean velocity (V_c) and velocity dispersion σ_c by using the galaxies with recessional velocities within $V_c \pm 3 \times \sigma_c$ and inside r_{200}. This iterative process stopped when no changes in V_c and σ_c from one step to the other was obtained. This process returns a total of 26 groups members with $m_r < 21.0$ and within r_{200}. Using these group members we obtain: $V_c = 15\,551 \pm 65$ km s^{-1} and $\sigma_c = 333 \pm 46$ km s^{-1}. The remaining 254 objects with radial velocities out from the $V_c \pm 3 \times \sigma_c$ range and within 4 Mpc from the group center will be called background galaxies.

Figure 2 shows the spectroscopic completeness (C) as a function of the r-band apparent magnitude (m_r). This completeness was obtained by $C = N_{vel}/N_{phot}$, where N_{vel} and N_{phot} represents the number of galaxies with measured velocities and the number of spectroscopic targets per magnitude bin, respectively (see Agulli et al. 2014). In addition, Fig. 2 also shows the fraction of cluster members (f_{mem}) as a function of m_r. This fraction is given by: $f_{mem} = N_{mem}/N_{vel}$, where N_{mem} shows the number of galaxy group members per magnitude bin (Agulli et al. 2014). The spectroscopic completeness is 100% for galaxies brighter than m_r = 16.6. This completeness slowly decreases to ~80% at $m_r \sim 19$, and ~25% at $m_r \sim 20.5$. The fraction of members decreases steeply with the magnitude. At m_r fainter than 18.0, less than 15% of the observed galaxies turned out to be group members. This indicates the low efficiency at faint magnitude for the selection of group members by a simple color cut.

Figure 3 shows the sky distribution of the spectroscopic targets, background galaxies, and member galaxies within r_{200} around the center of RX J075243.6+455653.

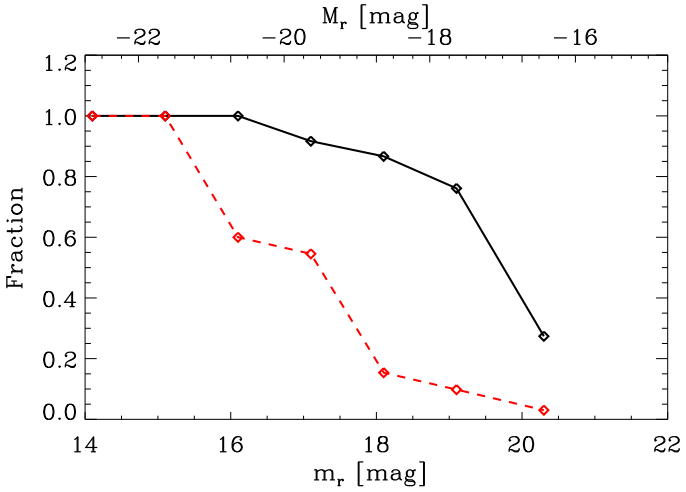

Fig. 2. Spectroscopic completeness (black) and fraction of group members (red dashed) as a function of the r-band magnitude.

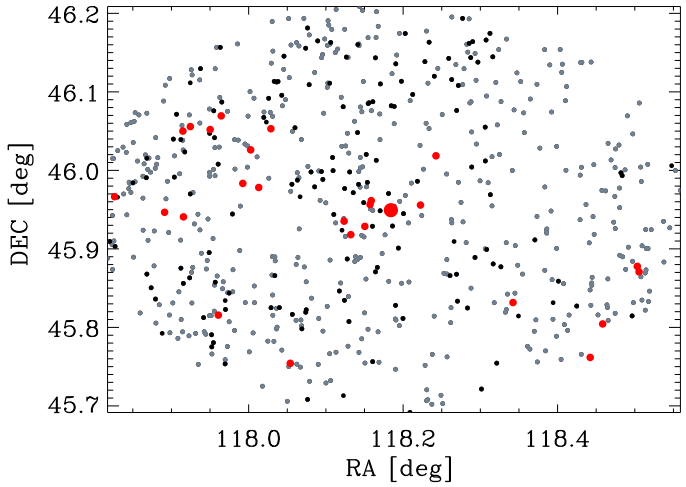

Fig. 3. Sky position of the spectroscopic targets (gray), background objects (black), and galaxy group members (red) within r_{200}. The largest red point represents the position of the brightest galaxy in the group.

3. Results

3.1. The fossilness of RX J075243.6+455653

Figure 4 shows the distance of the galaxies from the BGG as a function of their r-band apparent magnitude. According to the definition of fossil groups given by Jones et al. (2003), RX J075243.6+455653 is a fossil system. It shows a X-ray luminosity larger than 10^{42} erg s^{-1}, and the magnitude gap between the 1st and 2nd ranked galaxies within $0.5r_{200}$ is $\Delta m_{12} = 2.1$. Furthermore, the magnitude gap between the 1st and 4th ranked galaxies of the system within $0.5r_{200}$ is $\Delta m_{14} = 2.55$ (Zarattini et al. 2014), meeting the fossil criteria of Dariush et al. (2010).

There are several group members within $0.5 < R/r_{200} < 1.0$ with magnitudes similar to the BGG. Thus, these galaxies result in $\Delta m_{12} < 2$ within r_{200}. We can speculate that probably these galaxies are in the process of falling into the group, and will pass closer to the group center and merge with the BGG in the next few Gyr. This would imply that the fossilness of RX J075243.6+455653 is a transition state as reported by some cosmological simulations (von Benda-Beckmann et al. 2008; Kundert et al. 2017). The transitory nature of the fossil state has also been reported in some other observed systems in the literature (e.g., Zarattini et al. 2014).

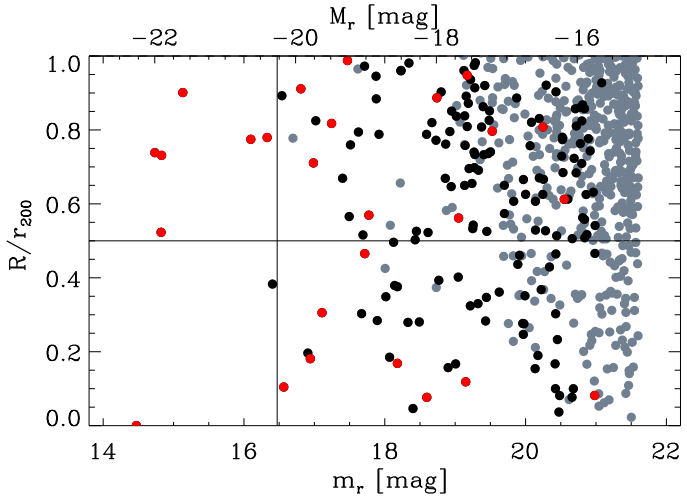

Fig. 4. Magnitude-distance diagram for the group RX J075243.6+455653. The distance to the BGG is shown as a function of the r-band magnitude for each galaxy within r_{200}. The gray, black, and red points represent the spectroscopic targets, background galaxies, and group members, respectively. The horizontal and vertical full lines represent $R/r_{200} = 0.5$ and $\Delta m_{12} = 2.0$, respectively.

According to the definition of fossil systems, the fossilness strongly depends on the adopted value of r_{200} of the structure. Figure 4 shows that changes in the value of r_{200} could change the fossillness of RX J075243.6+455653. The value of r_{200} for this group was determined from the X-ray luminosity obtained from RASS data. We have also computed r_{200} by using the velocity dispersion of the system and the relation: $r_{200} = \frac{\sqrt{3}\sigma_c}{10H(z_c)}$, where $H(z_c)$ is the value of the Hubble constant at the redshift of the group (z_c) (e.g., Carlberg et al. 1997; Aguerri et al. 2007). In this case we have calculated $r_{200} = 0.80$ Mpc, which is ∼17% smaller than the obtained from X-ray data. This difference could be related to the luminous AGN that the central galaxy of RX J075243.6+455653 hosts (see Kundert et al. 2015). Nevertheless, the fossilness of the system does not change with the new r_{200} computed (see Fig. 4).

We can also investigate whether or not the X-ray luminosity of the AGN would affect the fossilness definition of RX J075243.6+455653. Girardi et al. (2014) obtained a relation between the X-ray luminosity and the optical luminosity (L_{opt}) for a sample of clusters and fossil systems. According to this work, RX J075243.6+455653 shows an optical luminosity of $L_{opt} = 3.05 \times 10^{11}\ h_{70}^{-2}\ L_{\odot}$. Taking into account the Girardi's relation, RX J075243.6+455653 would have a X-ray luminosity of $L_X = 5.78 \times 10^{42}\ h_{70}^{-2}$ erg s^{-1}. This value is larger than $10^{42}\ h_{50}^{-2}$ erg s^{-1} chosen as limit to define fossil systems. Therefore, we can say that the fossillness of RX J075243.6+455653 is not compromised by the X-ray luminosity of the central AGN. We also note that the limit in the X-ray luminosity used to define fossil systems is taken in order to avoid isolated galaxies. In this case, the velocity dispersion of the system shows us that RX J075243.6+455653 is a group-like halo.

3.2. The color–magnitude diagram

Figure 5 shows the color–magnitude diagram of the galaxies located within r_{200} around the center of RX J075243.6+455653.

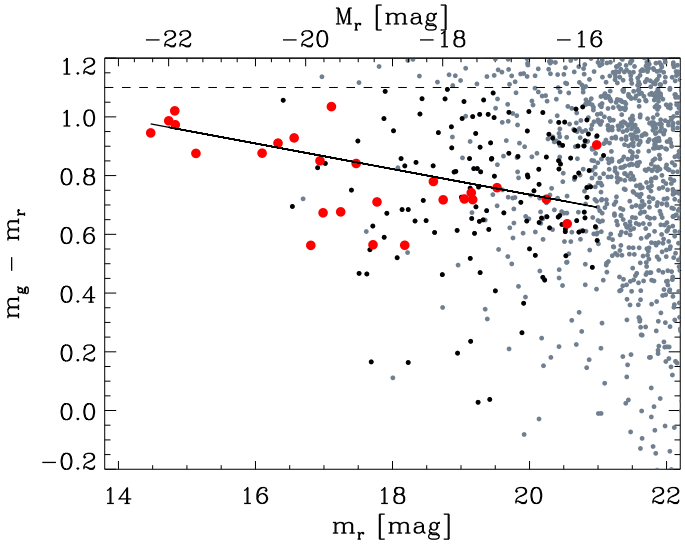

Fig. 5. Color–magnitude diagram of the galaxies within r_{200} from the group center. The gray points represent all the galaxies in the direction of the group. Red and black points show the group members and the background galaxies, respectively. The horizontal dashed line represents the color limit chosen for the selection of the spectroscopic targets. The full line shows the fitted red sequence.

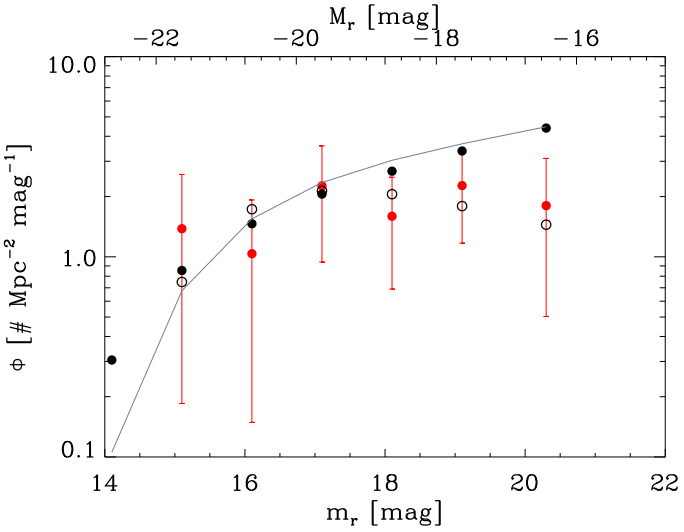

Fig. 6. Luminosity function of the galaxies within r_{200} from the group center (red points). The Schechter fits of the composite luminosity functions for systems with $\Delta m_{12} < 0.5$ and $\Delta m_{12} > 1.5$ from Zarattini et al. (2015) are also overplotted with filled and empty black circles, respectively. The gray full line represents the Schechter fit of the LF for groups with $\log(M) = 13.56$ from Zandivarez & Martínez (2011). All LFs have been normalized in the magnitude interval $14 < m_r < 18$.

We have fit the red sequence (RS) for those group members with $m_r < 18.0$ and with $g - r > 0.8$. The best fit is $(g-r)_{\rm RS} = -0.043 \pm 0.01 m_r + 1.606 \pm 0.20$ and $\sigma_{\rm RS} = 0.036$. Taking into account the errors of the fit of the red sequence, the intrinsic scatter is $\sigma_{RS,i} = 0.16$. The red sequence of the group is well defined down to the dwarf regime ($M_r \sim -16.0$).

We have divided the group members into red and blue galaxies. We have considered blue galaxies as those group members with $g - r < (g-r)_{\rm RS} - 3\sigma_{\rm RS}$, where $(g-r)_{\rm RS}$ and $\sigma_{\rm RS}$ are the color and the dispersion of the red sequence (see e.g., Agulli et al. 2014). We have obtained six groups members classified as blue galaxies, implying that the blue fraction of this group is 0.23. These blue galaxies are located in the external regions of the group, at a mean distance of $0.7 r_{200}$. This number of blue galaxies can be considered as an upper limit. No blue galaxies are obtained if we consider blue galaxias as those group members with $g - r < (g-r)_{\rm RS} - 3\sigma_{{\rm RS},i}$.

We also note the absence of blue galaxies fainter than $M_r \sim -18.0$. Although some blue galaxies have been spectroscopically observed in this magnitude range, they turned out be background objects. Due to the small number of observed galaxies, it is difficult to be certain of a lack of blue dwarf galaxies in this group.

3.3. The spectroscopic galaxy luminosity function

Figure 6 shows the spectroscopic galaxy LF of the group within r_{200}. This LF was computed as $\Phi(M_r) = N_{\rm phot}(M_r) \times f_{\rm mem}(M_r)/A$, where A is the area of the observations, $N_{\rm phot}$ is the number of photometric targets per magnitude bin, and $f_{\rm mem}$ is the fraction of group members per magnitude bin (see e.g., Agulli et al. 2014). The uncertainties were obtained by Poisson statistics.

Although the uncertainties of the LF are large, we can see that the faint-end is flat. We have fit the observed spectroscopic LF by a Schechter function. The reported faint-end slope was $\alpha = -1.08 \pm 0.33$. The large uncertainty in α results from the large observational errors in the LF. This slope is less steep than others from massive clusters ($\alpha \sim -1.5$; Agulli et al. 2014, 2016) or the field (Blanton et al. 2005). Nevertheless, the slope is similar within the uncertainties with the LF in groups of galaxies ($\alpha \sim -1.16$; Zandivarez & Martínez 2011) or some dynamically young massive clusters (($\alpha \sim -1.13$; Agulli et al. 2017).

The large uncertainty in the α parameter of the fitted Schechter function makes comparison with other samples difficult. In particular, we aim to compare the LF of the group with the composite LFs of Zarattini et al. (2015) for systems with small ($\Delta m_{12} < 0.5$) and large ($\Delta m_{12} > 1.5$) magnitude gaps. To avoid this problem, we have used the Pearson test. This statistical test reports that the LF of RX J075243.6+455653 can be modeled by the Schechter function fitted for systems with large magnitude gap ($\Delta m_{12} > 1.5; \chi^2 = 0.16$). However, the LF of systems with small Δm_{12} is not a good representation of the LF of RX J075243.6+455653 ($\chi^2 = 23.03$). In addition, the Pearson test also suggests that the Zandivarez & Martínez (2011) LF for systems with similar mass as RX J075243.6+455653 is not a good representation of our data ($\chi^2 = 10.05$). This analysis indicates that the LF of this group is similar to the LF of systems showing flat faint-end slopes, such as the systems with large magnitude gaps reported by Zarattini et al. (2015).

The flatness of the LF can also be reflected in the dwarf-to-giant ratio (DGR). This quantity measures the ratio between the number of dwarf and bright galaxies in clusters and groups. Following the definition from Popesso et al. (2006), we have considered dwarf galaxies as those members with $-18.0 < M_r < -16.5$, and bright group members as those with $M_r < -20.0$. The obtained DGR for the members within r_{200} for RX J075243.6+455653 was 0.99 ± 0.49, indicating that this group contains about one dwarf galaxy per giant.

3.4. The large-scale environment

We have analyzed the degree of isolation of RX J075243.6+455653 by searching in the NASA Extragalactic Database (NED) for galaxy systems within 2 degrees of the group center;

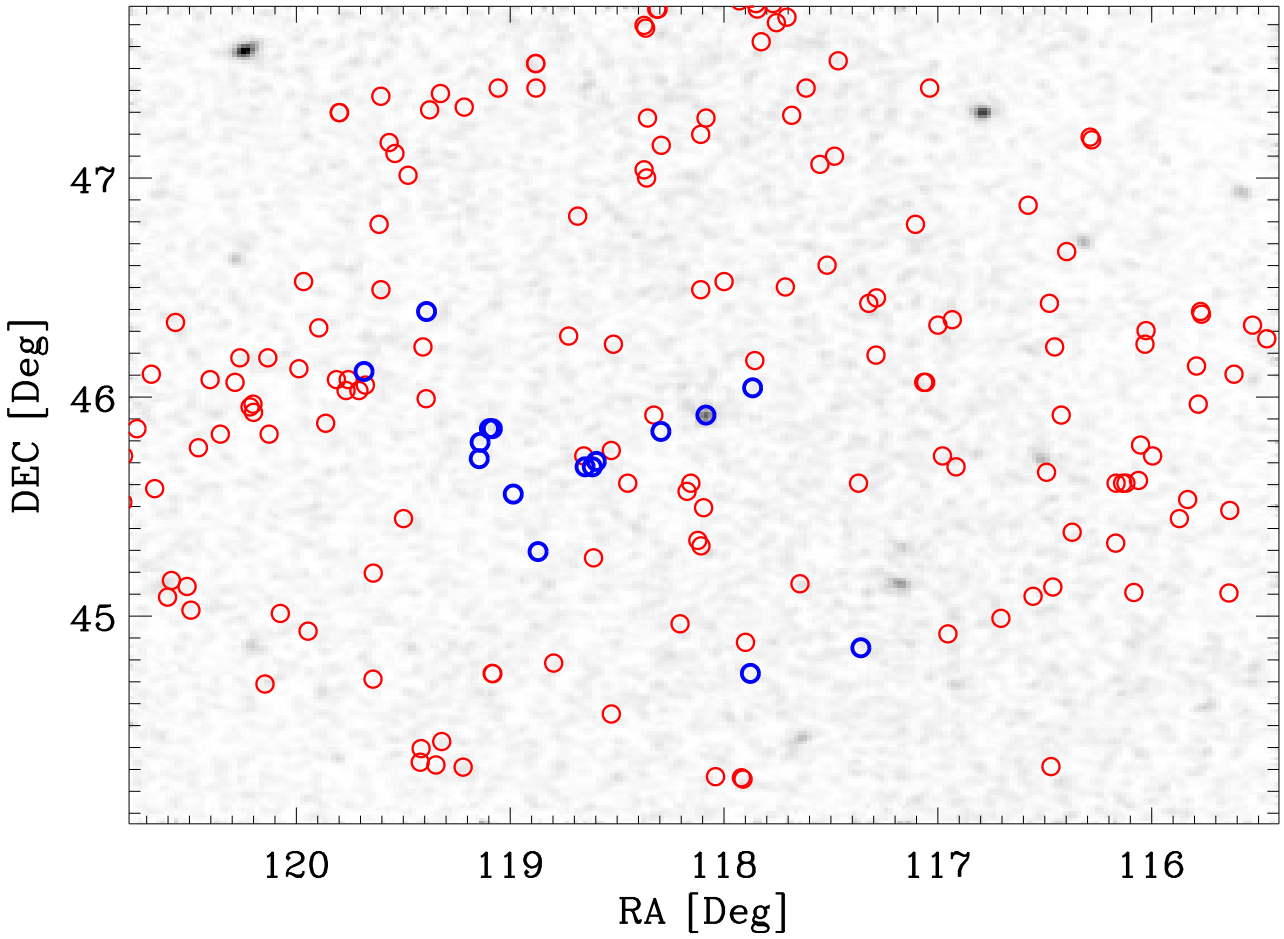

Fig. 7. ROSAT image centered at the position of RX J075243.6+455653. The open circles show the position of other groups and galaxy clusters reported by NED within 2 degrees from the group center. The red symbols represent objects with radial velocities larger than 18 000 km s^{-1} or smaller than 12 000 km s^{-1}. Blue circles show groups with radial velocities in the range 12 000 $< V <$ 18 000 km s^{-1}.

corresponding to a search radius of ∼7.2 Mpc at the distance of the group. Sixteen galaxy aggregations with radial velocity in the range 12 000 $< V <$ 18 000 km s^{-1} were found in this search, with 15 of them located within $\pm 3\sigma_c$ from the central radial velocity of RX J075243.6+455653. In addition, two of these groups are located at a projected distance from the group center smaller than r_{200}. The data obtained from NED are heterogeneous. Nevertheless, NED has one of the largest datasets on clusters and groups of galaxies. The 16 galaxy aggregations retrieved from the NED database come from six sources in the literature. They were obtained from data of large galaxy surveys as SDSS (Smith et al. 2012; Berlind et al. 2006; Miller et al. 2005; McConnachie et al. 2009) and the Two Micron All-Sky Survey (2MASS; Díaz-Giménez & Zandivarez 2015; Crook et al. 2007). We have not identified groups or clusters within 2 degrees of the group center and with $V <$ 20 000 km s^{-1} in other large cluster surveys as maxBCG (Koester et al. 2007), WHL (Wen et al. 2009), or RedMaPPer (Rykoff et al. 2016).

Figure 7 shows the position on the sky of the galaxy groups and clusters obtained from NED in a search radius of 2 degrees around the group center. The objects with radial velocities in the range 12 000 $< V <$ 18 000 km s^{-1} are located in a filamentary structure which extends for several Mpc. In contrast, the background groups are more randomly distributed. Figure 8 represents the conical diagrams with the position of RX J075243.6+455653 and the other groups.

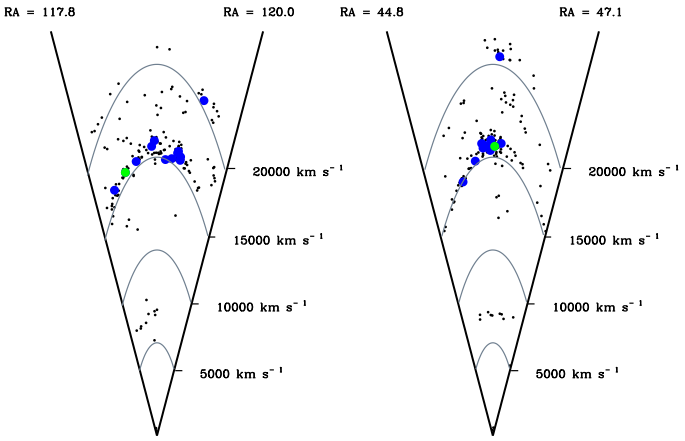

Fig. 8. Conical diagrams for the RX J075243.6+455653 group (green point) and other galaxy groups (blue points). The black points represent galaxies with $V <$ 22 000 km s^{-1}. The gray lines shows the iso-velocity curves corresponding to 5000, 10 000, 15 000, and 20 000 km s^{-1}.

This plot shows clearly that most of the groups have a similar radial velocity as RX J075243.6+455653. We can conclude that RX J075243.6+455653 is not an isolated structure. Indeed, this group forms part of a large and rich structure of groups of galaxies located within a radius of ∼7.2 Mpc from the

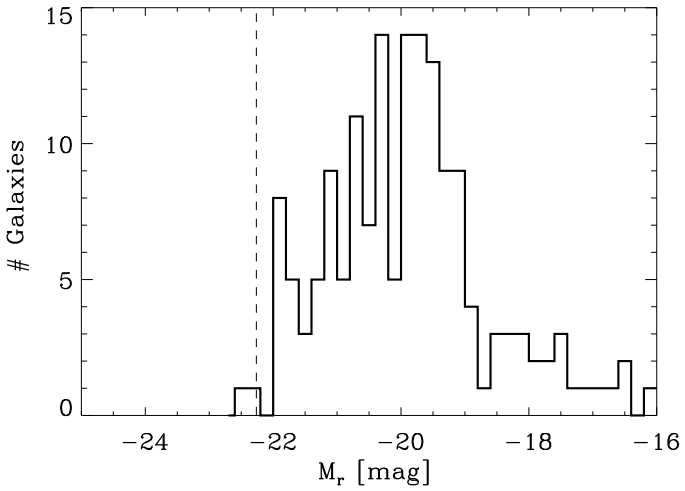

Fig. 9. Absolute r-band magnitude of the galaxies within 2 degrees from the center of RX J075243.6+455653 and with $|V - V_c| < 3\sigma_c$. The vertical dashed line represent the absolute magnitude of the BGG of RX J075243.6+455653.

group center. The filamentary distribution of the nearby groups could indicate that they are falling into the potential well of RX J075243.6+455653.

Figure 9 shows the absolute magnitude histogram of the galaxies located within 2 degrees from the center of RX J075243.6+455653 and with $|V - V_c| < 3\sigma_c$. The central galaxy of RX J075243.6+455653 is the second brightest object in this region of the sky. There is another galaxy 0.14 mag brighter and located at 2.5 Mpc from the center of RX J075243.6+455653. We can consider that these two galaxies are the dominant ones in the field. Figure 7 shows the X-ray emission image from the ROSAT satellite in which it can be seen that the group RX J075243.6+455653 is located in the X-ray peak in the center of the image. No other galaxy group from NED with $12\,000 < V < 18\,000$ km s^{-1} is associated with an X-ray peak that can be observed in the ROSAT image.

We can speculate that due to the bright luminosity of the BGG and its position at the peak of the X-ray, the RX J075243.6+455653 group is the dominant structure in this region of the sky. Then, the small groups of galaxies located around RX J075243.6+455653 would contribute to the hierarchical formation of this system. In addition, the bright galaxies could merge with the central galaxy of RX J075243.6+455653 increasing its luminosity, hence reinforcing its fossilness nature. The accretion of the different galaxy groups could also bring dwarf galaxies into the group and will increase the faint-end slope of the LF of RX J075243.6+455653.

4. Discussion

The results obtained in Sect. 3 indicate that RX J075243.6+455653 is not the remnant of an evolved and ancient group. In contrast, this galaxy aggregation is still in the hierarchical process of the accretion of its mass. Several facts related with the large scale environment and the faint-end slope of the spectroscopic LF of this group confirm this main result.

4.1. The dwarf galaxy population of RX J075243.6+455653

Dwarf galaxies in groups and clusters have valuable information about the mass assembly of the systems. There is still an open debate over the formation of the dwarf population in galaxy aggregations. There is some dynamical evidence that at least a fraction of dwarf galaxies residing in galaxy clusters today were not formed within the cluster (e.g., Conselice et al. 2001). In contrast, they were accreted into the clusters over several Gyr (Adami et al. 2007; Aguerri et al. 2017), or could be produced by the disruption of brighter galaxies due to strong tidal interactions between galaxies or with the cluster potential (e.g., Popesso et al. 2006; Aguerri 2016).

The faint-end slope of the galaxy LF indicates the density of the dwarf galaxy population. It depends on many cluster properties such as the dynamical relaxation of the cluster (López-Cruz et al. 1997; Agulli et al. 2017) or the mass of the halo (Zandivarez & Martínez 2011). The LF in groups of galaxies seem to be flatter than those in clusters. Zandivarez & Martínez (2011) found, for a large sample of galaxy groups and clusters from SDSS-DR7, a dependence between the mass of the halo and the faint-end slope of their LFs. In particular, for halos of masses similar to RX J075243.6+455653 they obtained $\alpha = -1.16$. The Pearson test indicated that the Zandivarez & Martínez (2011) LF was not a good representation of our data. In contrast, according to this statistical test, the LF of this group is similar to systems showing flatter faint-end slopes in their LFs as those with large magnitude gaps reported by Zarattini et al. (2015). This implies that RX J075243.6+455653 shows a flatter LF than groups with similar mass, and therefore, the density of dwarfs in RX J075243.6+455653 is smaller than in groups with similar mass.

The DGR is a statistic to compare the number of dwarfs per giant galaxy between different clusters or groups. Popesso et al. (2006) shows that the DGR measured within r_{200} is independent of the cluster or group mass. We have computed that the DGR of RX J075243.6+455653 is 0.99 ± 0.49. This number is one of the smallest values reported by Popesso et al. (2006) for a set of groups and clusters. This also points towards RX J075243.6+455653 having a lower density of dwarf galaxies in comparison with other systems with similar mass.

Several scenarios could explain the lack of dwarfs observed in RX J075243.6+455653. It could be related with the accretion status of the system. In particular, the low number of dwarfs in RX J075243.6+455653 might indicate that this system is still accreting the dwarf galaxy population. The accretion of the groups in its nearby environment will increase the number of dwarfs in the system.

RX J075243.6+455653 has a well defined red sequence down to the dwarf regime. Indeed, all dwarf galaxies of this system were found to be red with no detection of blue dwarf galaxies. Galaxy clusters at $z \sim 0.8-1.0$ have been found to show a lack of red dwarf galaxies (De Lucia et al. 2007); and this later formation of the red sequence in the dwarf regime in galaxy clusters indicates that the red dwarf population takes several Gyr to settle down. The fact that RX J075243.6+455653 already has red dwarf galaxies could indicate that this group was already formed several Gyr ago, where the red population of dwarf galaxies in the system are likely remnants of early accretion. Numerical simulations show that halos of groups of galaxies with masses similar to RX J075243.6+455653 have assembled half of their mass at $z \sim 1$ (Kundert et al. 2017). Nevertheless, the number of dwarfs of this system is low in comparison with other similar halos, which could indicate that this group is under the hierarchical process of its total mass accretion. The strong dynamical friction suffered by the luminous galaxies results in their merging with the group brightest galaxy on a short time scale. In contrast, the dynamical friction will be less effective on the dwarf accreted

population and will then not merge. This accretion process could decrease the number of luminous galaxies and increase the number of dwarfs. Then, the DGR of the system can increase by the accretion of nearby satellites into the group.

The lack of dwarfs shown by this group can also be explained as a consequence of a destruction of low-mass halos in this system. This galaxy disruption could be due to interactions with the group potential or other galaxy group members (e.g., Popesso et al. 2006; Aguerri 2016). The low velocity dispersion of the system would favor low-velocity interactions that make stripping of stars from low-mass galaxies more efficient, making them fainter (e.g., Mastropietro et al. 2005; Aguerri & González-García 2009; D'Onghia et al. 2009, 2010). In contrast, the low mass of the halo of RX J075243.6+455653 makes it difficult to follow the hypothesis of a massive destruction of dwarf galaxies by halo gravitational shocking (e.g., Mayer et al. 2002). It could also be that dwarf galaxies merge with the dominant galaxy of the system. The low-velocity dispersion of this group would favor this hypothesis. In addition, these minor mergers could transport some gas to the center of the main galaxy and contribute to the AGN feedback, which could explain the bright AGN associated with the central galaxy of RX J075243.6+455653. Indeed, Hess et al. (2012) found that the central galaxy of this group shows extended bipolar jets, as a consequence of this AGN activity.

4.2. The large-scale environment of fossil systems

Little is known about the large-scale environment around fossil and non-fossil systems. Only the environment of four fossil systems has been analyzed so far. The results are not conclusive because two of them seem to be embedded in dense large-scale environments and the other two appear isolated (Adami et al. 2007, 2012; Pierini et al. 2011). Numerical simulations show that FSs are embedded in denser environments at $z \sim 0.4$–0.7 than non-FSs. In addition, local FSs are located in slightly more under-dense regions than non-FSs (Díaz-Giménez et al. 2011; Dariush et al. 2010). Kundert et al. (2017) have shown that the difference between fossil and non-fossil systems identified at $z = 0$ is in the mass accretion of their dark matter halos over the past few Gyr. In particular, present-day FSs have assembled 80% of their mass at higher redshifts than non-FS. This suggests that the large-scale environment might be crucial for the evolution of the magnitude gap. Thus, systems embedded in dense environment could accrete a larger amount of their mass over smaller time-scales than those isolated. This accretion extended along several Gyr would make the fossilness a transitional stage. In addition, extended accretion would also allow for the central galaxies to increase their mass during a larger redshift interval.

The system RX J075243.6+455653 is embedded in a rich and complex large-scale structure formed by several groups of galaxies. There are 15 small galaxy groups within ∼7 Mpc around the group and with radial velocities within $V_c \pm 3\sigma_c$. This indicates that the region around RX J075243.6+455653 is rich in substructure. In addition, RX J075243.6+455653 is the dominant structure of this complex system as indicated by the brightest group galaxy located at a peak of X-ray emission with $L_X = 2.2 \times 10^{43}\ h_{70}^{-2}$ erg s^{-1} (Zarattini et al. 2014). No other surrounding group of galaxies is located at any other X-ray emission peak. This dominance indicates that RX J075243.6+455653 is surrounded by a massive dark matter halo, and the other nearby galaxy groups will probably fall into this group. This rich environment reveals that RX J075243.6+455653 is far from the end of the accretion of its mass.

The BGG of RX J075243.6+455653 has an absolute magnitude of $M_r = -22.67$, and is one of the less luminous BGGs in the sample of FSs analyzed by Zarattini et al. (2014). However, this galaxy can still grow by the accretion of the bright galaxies in the nearby environment due to dynamical friction. The galaxies 2 mag fainter than the BGG, located in the galaxy groups, and with $|V - V_c| < 3\sigma_c$, have a total luminosity of $L_r = 1.05 \times 10^{12}\ h_{70}^{-2}\ L_{r,\odot}$. All these stars around RX J075243.6+455653 could potentially produce a central BGG with $M_r = -25.43$. This new galaxy would be comparable in luminosity to the brightest galaxies observed in other fossil clusters and will produce in the future a system with a large magnitude gap (see Zarattini et al. 2014). Interestingly, this scenario for RX J075243.6+455653 is in contrast with the prediction from numerical simulations which find that FSs with faint central galaxies are dynamically old objects (see Raouf et al. 2014).

The accretion of galaxies as we propose here for RX J075243.6+455653 could be not so rare in fossil systems. Recent minor mergers have also been proposed to explain the complex structure of the hot intracluster medium of the fossil group NGC 1132. This system shows a disturbed and asymmetrical morphology of its hot gas. These observations can be explained considering a recent minor merger with a low impact parameter (Kim et al. 2017). The case of NGC 1132 shows that fossil systems can be rejuvenated by recent mergers of galaxies or groups. Other X-ray observations indicate that FSs show radial variation of their hot gas content and their gas clumping (Pratt et al. 2016). All these observations indicate that fossil systems are not dynamically evolved systems as was thought.

5. Conclusions

We have analyzed the properties of the fossil group RX J075243.6+455653. Our main results are as follows:

- We have obtained 26 galaxy group members down to $M_r = -16.0$ and within r_{200} from the group center. These members provide a mean radial velocity of the group of $V_c = 1551 \pm 65$ km s^{-1} and a dispersion $\sigma_c = 333 \pm 46$ km s^{-1}.
- We have obtained the spectroscopic LF of RX J075243.6+455653 down to $M_r = -16.0$ and within r_{200}. The LF was fitted by a single Schechter function giving a flat faint-end slope $\alpha = -1.08 \pm 0.33$. We have used the Pearson test in order to compare the LF of our group with other LFs from the literature. In particular, the Pearson test reports that the LF of RX J075243.6+455653 is statistically similar to the LF of systems with large magnitude gaps ($\Delta m_{12} > 1.5$) obtained by Zarattini et al. (2014). And furthermore, the LF of RX J075243.6+455653 is not statistically similar to the LF of systems with $\Delta m_{12} < 0.5$ (Zarattini et al. 2014) or groups of galaxies with similar mass (Zandivarez & Martínez 2011).
- The DGR within r_{200} is 0.99 ± 0.49. This value is low compared with the DGR of other groups and galaxy clusters. Both the faint-end of the LF and the DGR of RX J075243.6+455653 indicate that this group has a lack of faint galaxies compared with groups or clusters with larger Δm_{12} or similar halos mass.
- Our search of groups or clusters of galaxies in the nearby environment of RX J075243.6+455653 finds that this group is not isolated. In contrast, it is embedded in a dense region with up to 15 groups of galaxies located in a thin velocity layer of ±1000 km s^{-1} and within ∼7 Mpc from the group center.

– RX J075243.6+455653 is the dominant structure of its complex and rich nearby environment. This is confirmed by the evidence that the central BGG of the group is located at the peak of an extended X-ray emission. No other surrounding galaxy groups are located in any other X-ray peak. This could imply that the surrounding galaxy groups will probably merge with RX J075243.6+455653 in the next few Gyr.

The results obtained in this paper indicate that RX J075243.6+455653 is still in the process of assembling its mass. The groups of galaxies located in its nearby environment will merge in the next few Gyr. These mergers will produce a growth of the BGG and will increase the number of dwarf galaxies of the system. This indicates that although today RX J075243.6+455653 is a fossil system, it is not a remnant of an evolved and ancient group. The fossil phase of this system could just be a transition state.

RX J075243.6+455653 is a fossil system according to the observational definition of this type of system. Nevertheless, it is not a relic of a structure formed at high redshift, and the halo of this group is still accreting mass from the groups located in its dense nearby environment. RX J075243.6+455653 is an example showing that the selection of fossil systems by only large magnitude gaps between the first two ranked galaxies does not guarantee the selection of dynamically old galaxy aggregations. New criteria should be obtained in order to find real relics of the structure formation at high redshift. In the near future, we will continue analyzing the properties of the large-scale environment and the faint-end of the LF of other nearby fossil systems. These properties in combination with state-of-the-art cosmological numerical simulations will allow us to find new observables in order to obtain remnants of ancient galaxy aggregations.

Acknowledgements. J.A.L.A. and S.Z. want to thank the support of this work by the Spanish Ministerio de Economia y Competitividad (MINECO) under the grant AYA2013-43188-P. We thank Dr. R. Barrena for the assistance provided for the data reduction and analysis of the OSIRIS data. This research has made use of the Thirteen Data Release of SDSS, and of the NASA/IPAC Extragalactic Database which is operated by the Jet Propulsion Laboratory, California Institute of Technology, under contract with the National Aeronautics and Space Administration. The WHT and its service program are operated on the island of La Palma by the Isaac Newton Group in the Spanish Observatorio del Roque de los Muchachos of the Instituto de Astrofísica de Canarias. Based on observations made with the Gran Telescopio Canarias (GTC), installed at the Spanish Observatorio del Roque de los Muchachos of the Instituto de Astrofísica de Canarias, in the island of La Palma. This research has made use of the NASA/IPAC Extragalactic Database (NED) which is operated by the Jet Propulsion Laboratory, California Institute of Technology, under contract with the National Aeronautics and Space Administration.

References

Adami, C., Russeil, D., & Durret, F. 2007, A&A, 467, 459
Adami, C., Le Brun, V., Biviano, A., et al. 2009, A&A, 507, 1225
Adami, C., Jouvel, S., Guennou, L., et al. 2012, A&A, 540, A105
Adelman-McCarthy, J. K., Agüeros, M. A., Allam, S. S., et al. 2008, ApJS, 175, 297
Aguerri, J. A. L. 2016, A&A, 587, A111
Aguerri, J. A. L., & González-García, A. C. 2009, A&A, 494, 891
Aguerri, J. A. L., Sánchez-Janssen, R., & Muñoz-Tuñón, C. 2007, A&A, 471, 17
Aguerri, J. A. L., Girardi, M., Boschin, W., et al. 2011, A&A, 527, A143
Aguerri, J. A. L., Agulli, I., Diaferio, A., & Dalla Vecchia, C. 2017, MNRAS, 468, 364
Agulli, I., Aguerri, J. A. L., Sánchez-Janssen, R., et al. 2014, MNRAS, 444, L34
Agulli, I., Aguerri, J. A. L., Sánchez-Janssen, R., et al. 2016, MNRAS, 458, 1590
Agulli, I., Aguerri, J. A. L., Diaferio, A., Dominguez Palmero, L., & Sánchez-Janssen, R. 2017, MNRAS, 467, 4410
Arnaud, M., Pointecouteau, E., & Pratt, G. W. 2005, A&A, 441, 893
Berlind, A. A., Frieman, J., Weinberg, D. H., et al. 2006, ApJS, 167, 1
Blanton, M. R., Lupton, R. H., Schlegel, D. J., et al. 2005, ApJ, 631, 208
Böhringer, H., Schuecker, P., Pratt, G. W., et al. 2007, A&A, 469, 363
Carlberg, R. G., Yee, H. K. C., & Ellingson, E. 1997, ApJ, 478, 462
Conselice, C. J., Gallagher, J. S., III, & Wyse, R. F. G. 2001, ApJ, 559, 791
Crook, A. C., Huchra, J. P., Martimbeau, N., et al. 2007, ApJ, 655, 790
Dariush, A. A., Raychaudhury, S., Ponman, T. J., et al. 2010, MNRAS, 405, 1873
De Lucia, G., Poggianti, B. M., Aragón-Salamanca, A., et al. 2007, MNRAS, 374, 809
Díaz-Giménez, E., & Zandivarez, A. 2015, A&A, 578, A61
Díaz-Giménez, E., Muriel, H., & Mendes de Oliveira, C. 2008, A&A, 490, 965
Díaz-Giménez, E., Zandivarez, A., Proctor, R., Mendes de Oliveira, C., & Abramo, L. R. 2011, A&A, 527, A129
Domínquez Palmero, L., Jackson, R., Molaeinezhad, A., et al. 2014, Proc. SPIE, 9149, 91492J
D'Onghia, E., & Lake, G. 2004, ApJ, 612, 628
D'Onghia, E., Sommer-Larsen, J., Romeo, A. D., et al. 2005, ApJ, 630, L109
D'Onghia, E., Besla, G., Cox, T. J., & Hernquist, L. 2009, Nature, 460, 605
D'Onghia, E., Vogelsberger, M., Faucher-Giguere, C.-A., & Hernquist, L. 2010, ApJ, 725, 353
Eigenthaler, P., & Zeilinger, W. W. 2013, A&A, 553, A99
Girardi, M., & Mezzetti, M. 2001, ApJ, 548, 79
Girardi, M., Giuricin, G., Mardirossian, F., Mezzetti, M., & Boschin, W. 1998, ApJ, 505, 74
Girardi, M., Aguerri, J. A. L., De Grandi, S., et al. 2014, A&A, 565, A115
Gozaliasl, G., Khosroshahi, H. G., Dariush, A. A., et al. 2014, A&A, 571, A49
Harrison, C. D., Miller, C. J., Richards, J. W., et al. 2012, ApJ, 752, 12
Hess, K. M., Wilcots, E. M., & Hartwick, V. L. 2012, AJ, 144, 48
Jones, L. R., Ponman, T. J., Horton, A., et al. 2003, MNRAS, 343, 627
Kennicutt, R. C., Jr. 1992, ApJS, 79, 255
Khosroshahi, H. G., Ponman, T. J., & Jones, L. R. 2006, MNRAS, 372, L68
Khosroshahi, H. G., Ponman, T. J., & Jones, L. R. 2007, MNRAS, 377, 595
Khosroshahi, H. G., Gozaliasl, G., Rasmussen, J., et al. 2014, MNRAS, 443, 318
Kim, D.-W., Anderson, C., Burke, D., et al. 2017, ApJ, submitted [arXiv:1706.04609]
Koester, B. P., McKay, T. A., Annis, J., et al. 2007, ApJ, 660, 239
Kundert, A., Gastaldello, F., D'Onghia, E., et al. 2015, MNRAS, 454, 161
Kundert, A., D'Onghia, E., & Aguerri, J. A. L. 2017, ApJ, 845, 45
Kurtz, M. J., Mink, D. J., Wyatt, W. F., et al. 1992, Astronomical Data Analysis Software and Systems I, 25, 432
La Barbera, F., de Carvalho, R. R., de la Rosa, I. G., et al. 2009, AJ, 137, 3942
Lieder, S., Mieske, S., Sánchez-Janssen, R., et al. 2013, A&A, 559, A76
López-Cruz, O., Yee, H. K. C., Brown, J. P., Jones, C., & Forman, W. 1997, ApJ, 475, L97
Mastropietro, C., Moore, B., Mayer, L., et al. 2005, MNRAS, 364, 607
Mayer, L., Moore, B., Quinn, T., Governato, F., & Stadel, J. 2002, MNRAS, 336, 119
McConnachie, A. W., Patton, D. R., Ellison, S. L., & Simard, L. 2009, MNRAS, 395, 255
Mendes de Oliveira, C. L., Cypriano, E. S., & Sodré, L., Jr. 2006, AJ, 131, 158
Méndez-Abreu, J., Aguerri, J. A. L., Barrena, R., et al. 2012, A&A, 537, A25
Miller, C. J., Nichol, R. C., Reichart, D., et al. 2005, AJ, 130, 968
Pierini, D., Giodini, S., Finoguenov, A., et al. 2011, MNRAS, 417, 2927
Ponman, T. J., Allan, D. J., Jones, L. R., et al. 1994, Nature, 369, 462
Popesso, P., Biviano, A., Böhringer, H., & Romaniello, M. 2006, A&A, 445, 29
Pratt, G. W., Pointecouteau, E., Arnaud, M., & van der Burg, R. F. J. 2016, A&A, 590, L1
Proctor, R. N., de Oliveira, C. M., Dupke, R., et al. 2011, MNRAS, 418, 2054
Raouf, M., Khosroshahi, H. G., Ponman, T. J., et al. 2014, MNRAS, 442, 1578
Rykoff, E. S., Rozo, E., Hollowood, D., et al. 2016, ApJS, 224, 1
Santos, W. A., Mendes de Oliveira, C., & Sodré, L., Jr. 2007, AJ, 134, 1551
Smith, A. G., Hopkins, A. M., Hunstead, R. W., & Pimbblet, K. A. 2012, MNRAS, 422, 25
Sommer-Larsen, J. 2006, MNRAS, 369, 958
Trevisan, M., Mamon, G. A., & Khosroshahi, H. G. 2017, MNRAS, 464, 4593
Voevodkin, A., Borozdin, K., Heitmann, K., et al. 2010, ApJ, 708, 1376
von Benda-Beckmann, A. M., D'Onghia, E., Gottlöber, S., et al. 2008, MNRAS, 386, 2345
Wen, Z. L., Han, J. L., & Liu, F. S. 2009, ApJS, 183, 197
White, S. D. M., & Rees, M. J. 1978, MNRAS, 183, 341
Zandivarez, A., & Martínez, H. J. 2011, MNRAS, 415, 2553
Zarattini, S., Barrena, R., Girardi, M., et al. 2014, A&A, 565, A116
Zarattini, S., Aguerri, J. A. L., Sánchez-Janssen, R., et al. 2015, A&A, 581, A16
Zarattini, S., Girardi, M., Aguerri, J. A. L., et al. 2016, A&A, 586, A63
Zibetti, S., Pierini, D., & Pratt, G. W. 2009, MNRAS, 392, 525